www.czasopisma.pan.pl PAN POLSKA AKADEMIA NAUK www.journals.pan.pl

Oceanologia, 67 (4)/2025, 67407
Polish Academy of Sciences
Institute of Oceanology

https://doi.org/10.5697/KPCV6249

Perspectives of seasonal hydrography and water masses in Saudi waters of the Arabian Gulf

Mohamed Asharaf[1], V.M. Aboobacker[2,*], C.P. Abdulla[2], Thadickal V. Joydas[1], Karuppasamy P. Manikandan[1], M. Rafeeq[2], Abdulaziz Al-Suwailem[1], P. Vethamony[2]

Abstract

The hydrographic characteristics and water mass features of the Saudi waters of the Arabian Gulf (Persian Gulf) are less documented compared to neighboring regions. This study analyzed vertical profiles of temperature, salinity, and density collected from five transects with 555 stations in Saudi waters during five seasons. Although the data were collected during 2002–2003, they reveal notable hydrographic variability and features associated with Saudi waters. The sea surface temperature during late autumn and winter shows strong horizontal fluctuations between the northern and southern belts of the Saudi coast, while a high temperature plume is formed in the central coast during early summer. The central and northern coasts of Saudi Arabia have high concentrations of salinity induced by shallow embayments, while the impact of brine is limited to small areas in the vicinity of the outfalls. The presence of three water masses, namely, Indian Ocean Surface Water (IOSW), Arabian Gulf Water (AGW), and Bay Systems-induced Water (BSW), has been evident in this region; however, they co-occur only during spring, early summer, and summer in central and northern transects. The autumn and winter are characterized by the presence of AGW and BSW in all transects, while the IOSW was absent due to the mixing and by the opposing effects of shamal winds, which diminishes the inflow of IOSW. Nonetheless, the early summer and summer, with strong thermal stratification, exhibit the progression of IOSW up to the northern end of the Saudi waters.

Keywords

Seasonal hydrography; Intrusion of IOSW; Stratification; Vertical homogeneity; Arabian Gulf

[1] *Applied Research Center for Environment and Marine Studies, Research & Innovation, King Fahd University of Petroleum and Minerals, P. B. No. 391, Dhahran 31261, Saudi Arabia*

[2] *Environmental Science Center, Qatar University, P.B. No. 2713, Doha, Qatar*

***Correspondence**: vmaboobacker@qu.edu.qa (V.M. Aboobacker)

Received: 2 June 2025; **revised:** 4 September 2025; **accepted**: 30 September 2025

1. Introduction

The Arabian/Persian Gulf (hereafter, the Gulf) is situated within the extensive, arid landmass of East Asia and is bordered by high mountain ranges. This geographical position gives the Gulf a tropical climate in summer and a temperate climate during winter. Consequently, atmospheric temperature undergoes high seasonal fluctuations, which are rapidly transferred to the water column due to the shallowness of the Gulf. In the western Gulf, the sea surface temperature (SST) is as low as 11°C during winter and as high as 38°C during summer (Alosairi et al., 2020). The high rate of evaporation and very little precipitation increases the salinity of the Gulf waters, which generally ranges from 38 to 45 (Rakib et al., 2021). In both summer and winter, most evaporation occurs in two south embayments, to the east and west of Qatar, where the depths are less than 10 m for over 1000 km^2 (Sheppard, 1993). As a result, the temperature and salinity in regions such as the Gulf of Salwa, Manifa Bay, and Ad Dafi Bay become higher compared to that in the open sea (KFUPM/RI, 1990a,b,c). In the Gulf of Salwa, the salinity reaches up to 63.3 and temperature up to 40°C (Joydas et al., 2015; Al-Abdulkader et al., 2019).

The circulation in the Gulf is highly complex due to shallow depths in its major part, and is driven by thermohaline, wind, and tidal forces. Tides enter the Gulf through the Strait of Hormuz, propagate as Kelvin waves and progress in a counterclockwise pattern along the Iranian coast and along the Saudi Arabian coastline (Le Provost, 1983; Madah and Gharbi, 2022). In the western Gulf, tides are complex standing waves, and their dominant patterns vary from semidiurnal to diurnal by one or two amphidromic points located in the northwestern part (due to semidiurnal tide)

and in the central part (due to diurnal tide) (Reynolds, 1993; Siddig et al., 2019). The wind-driven currents are greatly influenced by the northerly/northwesterly shamal winds (Mussa et al., 2024). Studies reveal that the net surface flow along the Saudi Arabian coast is toward the southeast/east (Veerasingam et al., 2020 a,b, 2021a,b). The persistent southward wind stress sets up coastal currents along both the Arabian and Iranian coasts (Johns et al., 1999). The southerly current causes downwelling along the Saudi coast and upwelling along the Iranian coast (Hassanzadeh et al., 2011). The flow along the Iranian coast seems to continue into the southeastern basin, up to the Strait of Hormuz as a tightly trapped coastal current. Freshwater input from the Iraqi Shatt-al-Arab system is expected to amplify the Saudi-Qatar-Emirate coastal current (KFUPM/RI, 1990a).

The high evaporation over the Gulf leads to an inverse estuarine circulation with high saline water leaving the Gulf through the deep part of the Strait of Hormuz and replaced by a less saline surface inflow from the Sea of Oman (Swift and Bower, 2003; Pous et al., 2013; de Marez et al., 2019). The thermohaline forcing is generally aroused by the sinking of dense water in the northern Gulf, and a persistent thermal front across the Gulf was found north of Qatar related to the thermohaline exchange through the Strait of Hormuz (Johns et al., 1999). The front is most intense in summer and weakest in the late winter and spring. The data suggests that the location of the front is linked to the penetration of comparatively less saline oceanic inflow into the Gulf (Rakib et al., 2021; Al-Ansari et al., 2022). Much of this inflow terminates in a counterclockwise flow east of the mid-Gulf front.

The sea surface salinity (SSS) of the Gulf increases as it moves from the mouth of the Gulf inwards (Thoppil and Hogan, 2010). Sinking of saltier and denser water starts in the northwestern part of the Gulf. The dense saline water migrates down south and increases the salinity of deeper water. There is an inflow of less saline water through the Strait of Hormuz along the Iranian coast, which is either weakened by the northwest shamal winds or sufficiently strengthened in the summer to reach the northern part of the Gulf. A cyclonic eddy is noted in the southern Gulf along with a cyclonic eddy in the northwest Gulf maintained by river runoff from the Shatt-al-Arab (Thoppil and Hogan, 2010). A southward coastal jet is tracked between the head of the Gulf and Qatar (Hunter, 1986; Reynolds, 1993). A recent study identified small-scale seasonal eddies in the Gulf of Salwa and in Qatar waters (Hanert et al., 2023). Reynolds (1993) reported that the surface residual flow is southeastward along both the Saudi and Iranian coasts. In the middle, between these two coasts, surface velocities appear to be much smaller than near the coasts and there is evidence that this part of the area shows almost zero net surface flow (Kämpf and Sadrinasab, 2006).

Studies point out that there are considerable variations in hydrography in the Gulf – both spatially and temporally, based on limited measurements. For instance, hydrography of the Qatar waters was studied based on a few transects measurements across the Exclusive Economic Zone (EEZ) in different seasons (Rakib et al., 2021; Al-Ansari et al., 2022; Elobaid et al., 2022; Aboobacker et al., 2024). Different water masses have been distinguished in the Qatari deep and intermediate waters from these studies. The intrusion of less saline Indian Ocean Surface Waters (IOSW) was clearly eident off the east coast of Qatar. However, the extension of these waters along the central axis of the Gulf and their presence in the Saudi Arabian coast are not well understood. Moreover, the anthropogenic and natural fluxes originating from the land masses will influence the distribution of hydrographic parameters in Saudi coastal waters.

The hydrography of Saudi Arabian territorial waters in the Gulf has been relatively understudied, primarily due to the unavailability of measured data for scientific research. A notable exception is the work of John et al. (1990), who conducted in situ observations at 15 stations along the Saudi Arabian coast and offshore, extending from southern Gulf of Salwa to Safaniya near the Kuwait border during 1985–1988. While their study provided useful insights on the hydrography of the region, the spacing between their stations was considerably wider. This limits the understanding of fine scale details of hydrography along the Saudi coast. In addition, reanalysis data available and the spatial resolution of numerical modeling excercises carried out in the region are coarse. In this context, the present study has been framed to evaluate the hydrography of the Saudi Arabian waters in the Gulf based on historical data. Although old, the data is vast, which constitutes five transects and large number of data points in different seasons. Spatial and seasonal variability has been assessed, and the physical drivers that causes the variability have been evaluated.

2. Area of study

The study area encompasses the Saudi Arabian waters of the Gulf, extending from Khafji (28.5°N, 48.5°E) in the north to Ras Tanura (27.7°N, 50.1°E) in the south (Figure 1). This region covers approximately 250 km along the coast and 100 km offshore, with water depths ranging between 2 to 65 m. Ras Tanura is situated at the mouth of the Gulf of Salwa – an extremely hypersaline water body in the Gulf. This hyper saline water has not been traced further north of Ras Tanura (John et al., 1990). The bathymetry of the study region is characterized by complex features including coral reefs. The shore-parallel depths are not entirely isoline. Various industries are located along the coast, including oil and gas facilities, desalination plants and thermal plants. In addition, a few aquaculture facilities are operated along this coastal belt. The central region, Jubail, is home to some massive desalination plants and

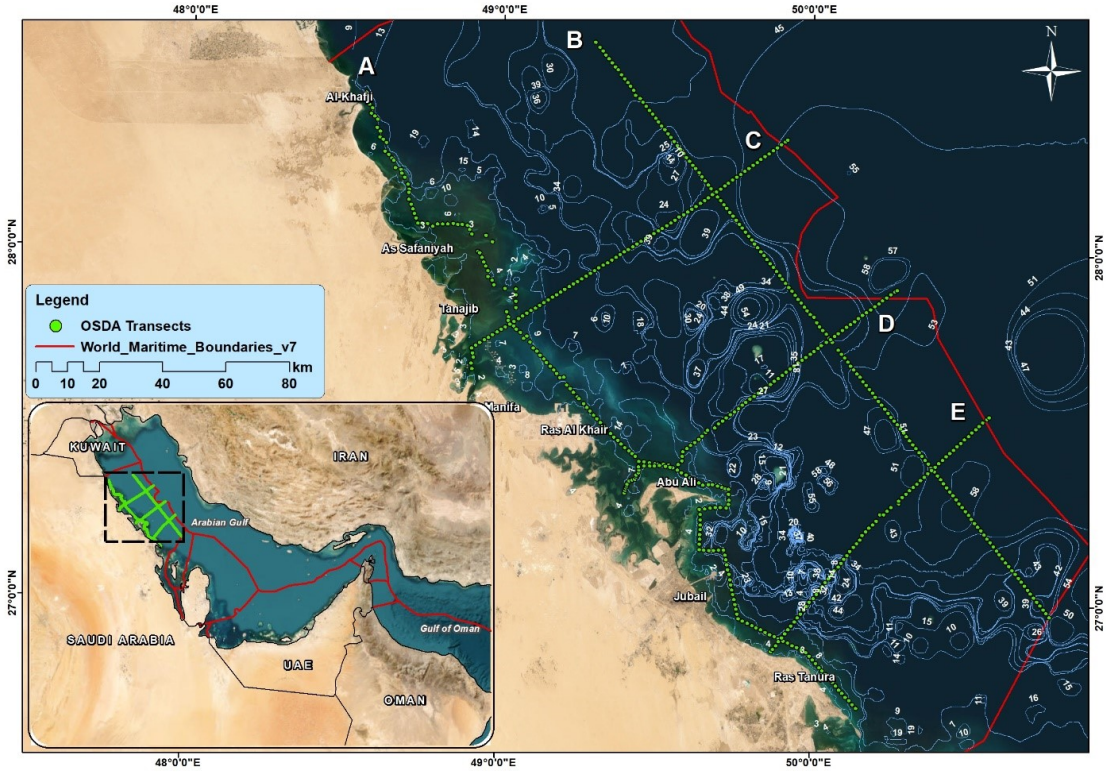

Figure 1. Transects of hydrographic measurements overlaid with bathymetric contours. The Saudi offshore boundary is marked in the red line. Inset: Arabian Gulf with sea boundaries of the Gulf countries and measurement transects.

is a major player in the world of water desalination with approximately 2,078,560–2,578,560 m^3 day^{-1}. There are a few shallow embayments north of Jubail Port, including Tanajib-Manifa-Ras Al Khair-Dohat Ad Dafi Bay systems and the semi-enclosed area bounded by Abu Ali Island.

Considering the climatic conditions of the Gulf, the seasons are broadly classified into summer (May–October) and winter (November–March) (Aboobacker et al., 2021a). The winter experiences stronger winter shamal winds (Aboobacker et al., 2021b) blown from the north/northwest direction. The summer shamal winds, with relatively lower frequency of occurrence also occur in this region. The Gulf also experiences other wind systems such as Nashi, Kaus and Suhaili winds (Aboobacker et al., 2021c). Large waves in the Gulf are characterized by shamal and nashi winds.

3. Data and methods

Five multi-disciplinary cruises were planned and executed to delineate the hydrography of the Saudi waters of the Gulf. Five transects (Table 1) with 555 stations were established for the measurements. The alongshore transects, running roughly in a northwest-southeast direction, have been classified as coastal waters (transect A) and offshore waters (transect B), while the cross-shore transects have been distinguished as northern waters (transect C), central waters (transect D) and southern waters (transect E). Transect A lies between the Kuwait border and Dammam, which follows the 5 m bathymetry line in 291 km length. Transect B lies between Karan Island and Arabiyah Island, extending from the Kuwait border to the Bahraini border, following a particular depth contour of 230 km length. The water depths are less than 15 m around the coastal transect, while they are between 25 m and 50 m in the offshore transect. Transect C is in the Tanajib area, with a length of 127 km; transect D is in the Abu Ali area, with a length of 120 km, and transect E is in the midway of Ras Tanura and Jubail, with a length of 103 km. The water depths along these cross-shore profiles vary roughly between 2 m and 55 m.

The sampling was carried out at each station once in each season, although it took a few days or weeks to complete the sampling. Given that it is difficult in practice to sample all the 555 stations at once (within 1 or 2 days), large differences in the dynamics are not expected in a few days' time, considering the inter-seasonal variability. The entire datasets have been used for generating spatial contours along the Saudi coast.

Oceanographic cruises were conducted on five transects during 2002–2003 (Table 1). Vertical profiles of temperature, salinity, and pressure have been measured at each station using the Sea-Bird SBE 25 SEALOGGER CTD.

Table 1. Geographical coordinates of the cruise transect lines.

Transect	Region*	Start		End		Cruise dates
		Latitude	Longitude	Latitude	Longitude	
A	Coastal	28°26′N	48°32′E	26°40′N	50°12′E	Late autumn: 14 November–13 December 2002
B	Offshore	28°36′N	49°17′E	26°56′N	50°48′E	Winter: 31 December 2002–19 January 2003
C	Northern	27°38′N	48°56′E	28°19′N	49°54′E	Spring: 15 April–06 May 2003
D	Central	27°19′N	49°24′E	27°53′N	50°14′E	Early summer: 31 May–17 June 2003
E	Southern	26°52′N	49°32′E	27°31′N	50°33′E	Summer: 14–30 August 2003

The density has been calculated based on the in situ temperature, salinity and pressure. Although the SBE-25 sensors were factory-calibrated, the quality of the CTD sensors were maintained by periodic calibrations. In total, 2775 profiles were taken for the entire study period. The SBE-25 CTDs were used earlier in the Gulf waters to measure the hydrography and analyzed the spatial and temporal variability (Rakib et al., 2021; Al-Ansari et al., 2022; Elobaid et al., 2022). The in situ data used in this study is made freely available to the public through Figshare (Asharaf et al., 2025). Ocean data plotting and analysis were carried out using Ocean Data View (ODV, mp-version 1.4-2003) (Schlitzer, 2003). Three interpolation methods are available in ODV, namely Quick gridding, Weighted-average gridding, and DIVA (Data-Interpolating Variational Analysis) gridding. The spatial interpolation in this study was performed by a weighted-average gridding technique. The data were gridded onto a regular grid with a varying grid resolution, depending on the data density. For each grid point, the interpolated value was calculated as a distance-weighted average of data from nearby stations. The results have been used to study the water constitution as well as distribution and to evaluate the spatial and seasonal variability of temperature, salinity, and density.

4. Results and discussion

4.1 SST, SSS, and SSD along the coastal transect

Seasonal variability of SST, SSS, and sea surface density (SSD) along the Saudi Arabian coast in the Gulf has been assessed by analyzing the data along Transect A (Figure 2). The winter exhibits the lowest SST, of the order of 15.6–20.9°C, followed by the spring, of the order of 21.6–24.7°C (Figure 2a). The SST during the late autumn and the early summer are 21.2–27.2°C and 28.2–30.4°C, respectively. Whereas the highest SST is found during summer, of the order of 33.2–34.9°C. The SST within the season, especially during late autumn and winter, indicate strong horizontal fluctuations between the coastal belt, with the lowest in the northern belt and highest in the first half of the southern belt. This is because during cold seasons, the shallow embayments in the north are colder than the surrounding regions, while the discharges from desalination plants may cause an increase in seawater temperature in the south. This is consistent with John et al. (1990) who reported the highest SST near Abu Ali Island, and Joydas et al. (2011) who noticed elevated temperatures in the shallow embayments of Manifa-Tanajib Bay system. Moreover, the difference between ambient and discharge temperatures is normally high during winter. Roy et al. (2022) estimated an average temperature difference between the intake and outfall of 3°C in cool weather seasons. This is consistent with the variations obtained here. On the other hand, there is no significant horizontal variation in SST during summer, as the outfall temperature did not make a considerable difference to the ambient temperature.

The overall annual range of SSS observed along the coastal transect is 40.0–43.8 (Figure 2b). Based on a numerical modeling study, Hassanzadeh et al. (2011) reported a range of salinities 39.0–41.5 along the Saudi coast. This has a slight underestimation with the values we obtained in the present study, which is primarily because the spike effects of the outfalls are not well replicated because of the coarse resolution of the model. The SSS is relatively low during late autumn and winter compared to the other seasons, while the difference is limited to a maximum of 2. Horizontal variations are evident from the northern coast to the southern coast of Saudi Arabia with spikes at a few stations, especially near the shallow embayments of northern coast. The higher salinities are mainly contributed from the shallow embayments, where the evaporation is much higher than the adjacent regions and the flushing is poor (Joydas et al., 2011). The dispersion of brine around Jubail desalination plants can also be taken into account in this salinity increment, because the coastal transect is not far from the outfall locations. The topography of the region suggests an obstruction for the northward movement of brine-induced water by the Abu Ali Island. This also added to the elevated salinity levels around this island. The southern coast has relatively low salinity compared to the northern coast. This region may act as a shadow zone with less impact from the surrounding coastal waters, but greater influence of the offshore waters. Along the east coast of Qatar, SSS of 39.0–41.5 were measured, with the lowest during summer and the highest during autumn (Al-Ansari et al., 2022). Measurements along the central transect of the Gulf show an SSS range of 37.3–41.4 (Ghaemi et al., 2022), which is lower than that found along the coastal regions. Coastal regions of the Gulf exhibit high salinities due to relatively high evaporation and the effect of desalination plants (Ibrahim et al., 2020). The measured

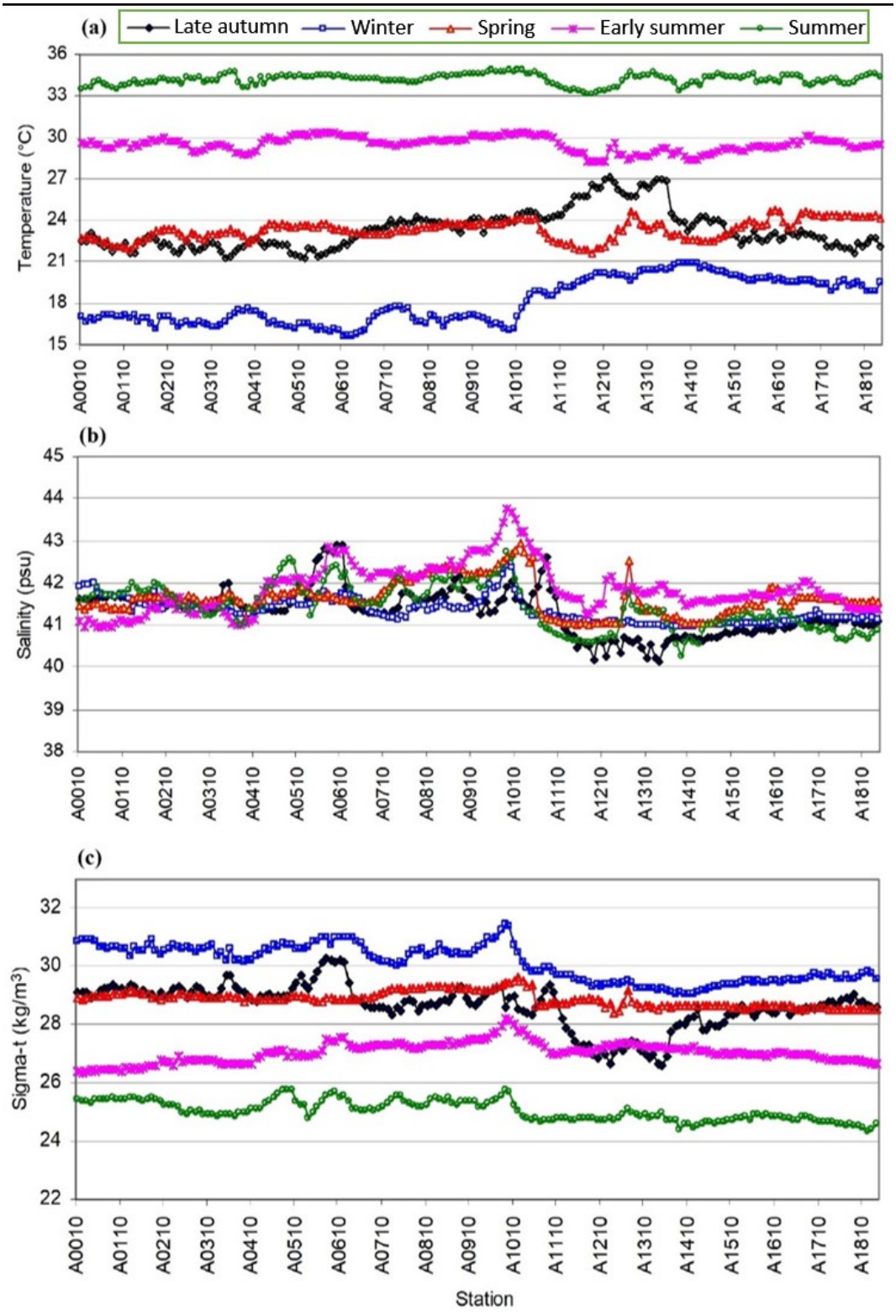

Figure 2. Distribution of sea surface temperature (a), sea surface salinity (b), and sea surface density (c) along the Transect A .

SSS in Kuwait Bay (43.0–44.5, Pokavanich et al., 2013) is higher than that measured along the Transect A, however, the coasts around the Gulf of Salwa have always been the highest salinity (above 60) of the Gulf (Joydas et al., 2023).

A north to south gradient exists in the SSD, except during early summer (Figure 2c). Although the magnitudes are small, these horizontal gradients can lead to a flow toward the south. This contributes to the Arabian Coastal Current (ACC) as evident from recent studies (Alosairi and Pokavanich, 2017; Mussa et al., 2024). However, the Abu Ali in the central coast restricts the nearshore flow of dense water toward the southeast. Within the existence of north-south gradients, there are some spikes of higher density at a few stations along the transect. During early summer, the density increases from the north until it meets the spike in the central coast. This is mainly attributed to the influence of hypersaline and high temperature waters of the shallow embayments along the northern coasts of Saudi Arabia (John et al., 1990; Joydas et al., 2011). Seasonal variability is evident in the sigma-t, with the lowest during summer (24.292–25.914 kg m^3) and the highest during winter (29.059–31.472 kg m^3). These are consistent with the SSS measured along the east coast of Qatar (Rakib et al., 2021; Al-Ansari et al., 2022).

4.2 Spatial distribution of SST, SSS, and SSD in Saudi waters

Considering all the transects (A, B, C, D, and E), spatial interpolation of SST, SSS, and SSD have been carried out using Ocean Data View for five seasons and presented in Figures 3, 4 and 5, respectively. The lowest SST is found during winter, with distinct horizontal variability (Figure 3b). The SST on the northern coast is about 15–17°C, while that on the southern coast is about 18–19°C, and the offshore is about 21–22°C. In the central region, the SST during winter is about 17.5–19.5°C, which is consistent with the observations of John et al. (1990). The offshore-nearshore gradient (lowest SST near the coast) is because the air-sea interaction is quite rapid along the coast due to shallow depths, where the air during winter is much cooler than the seawater temperature. This distribution of cooler waters in the nearshore is stronger in the midlatitudes and weaker in equatorial regions (Marin et al., 2021). The northern coast of Saudi Arabia is bounded by the deserts, while the southern coast is situated near the urban/industrial areas. An obvious temperature gradient between the desert and urban/industrial areas is reflected in the nearshore SST differences. A low- temperature plume is also visible on the central coast, affected by a discharge from the desalination plants in Jubail, which will have a lower temperature than seawater temperature during winter.

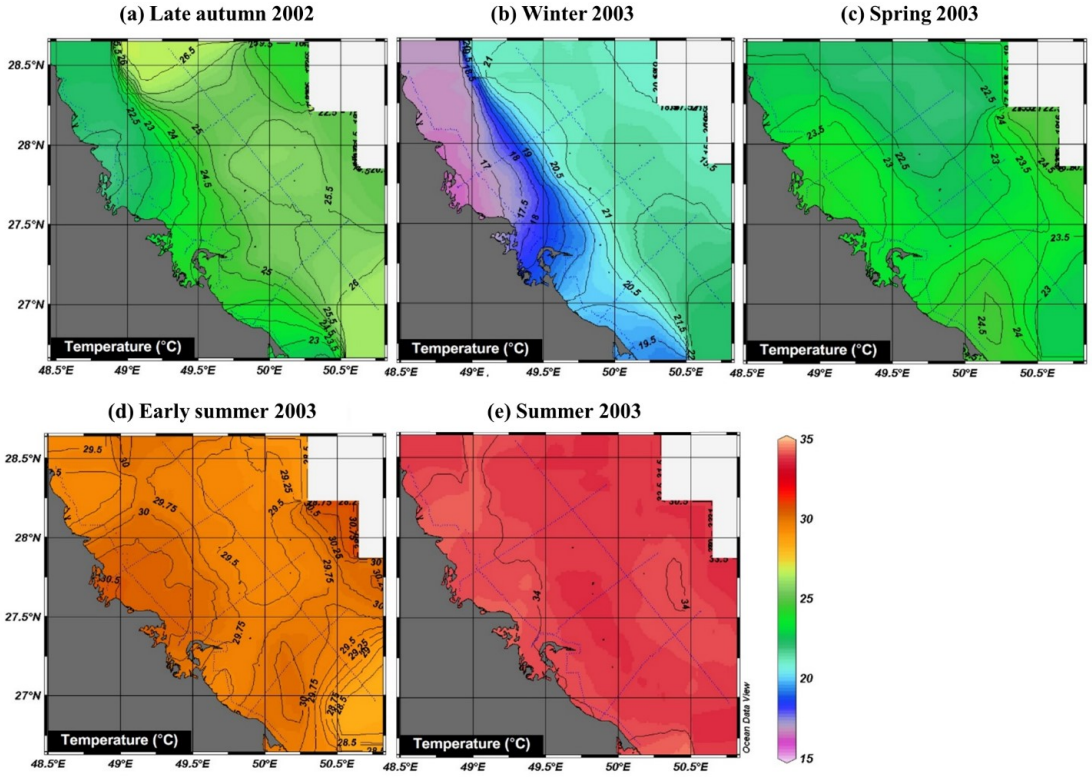

Figure 3. Spatial distribution of sea surface temperature in Saudi waters of the Gulf during late autumn 2002 (a), winter 2003 (b), spring 2003 (c), early summer 2003 (d) and summer 2003 (e).

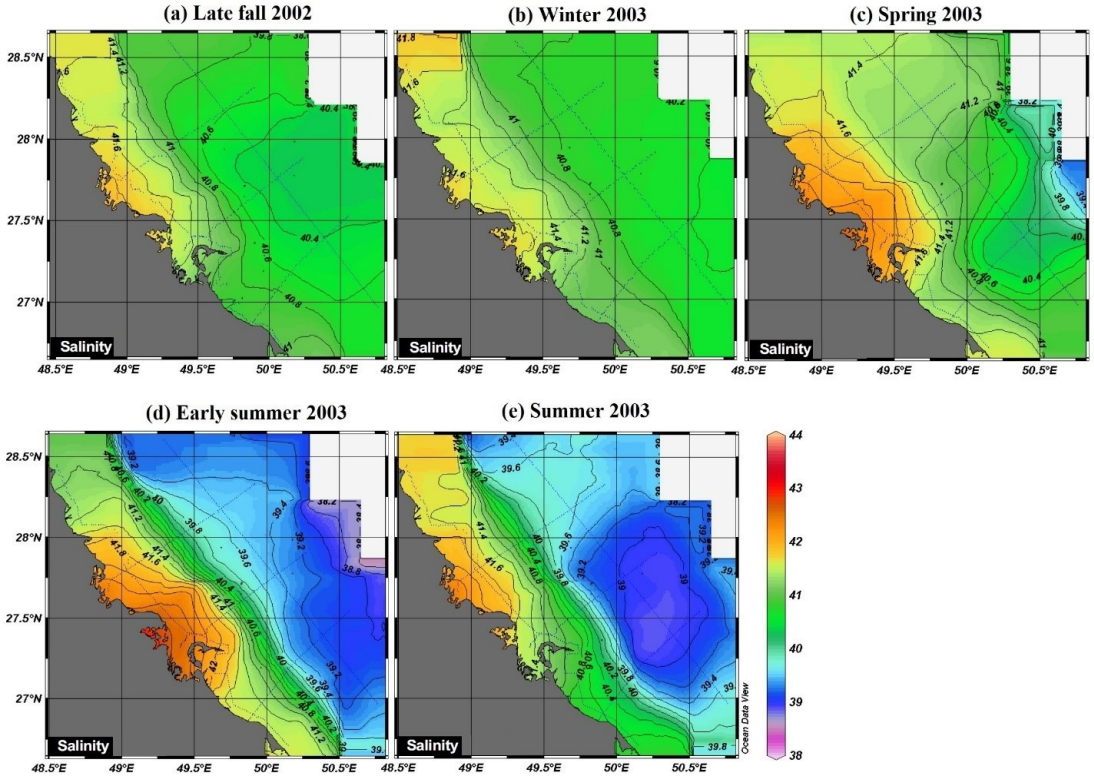

Figure 4. Spatial distribution of sea surface salinity in Saudi waters of the Gulf during late autumn 2002 (a), winter 2003 (b), spring 2003 (c), early summer 2003 (d) and summer 2003 (e).

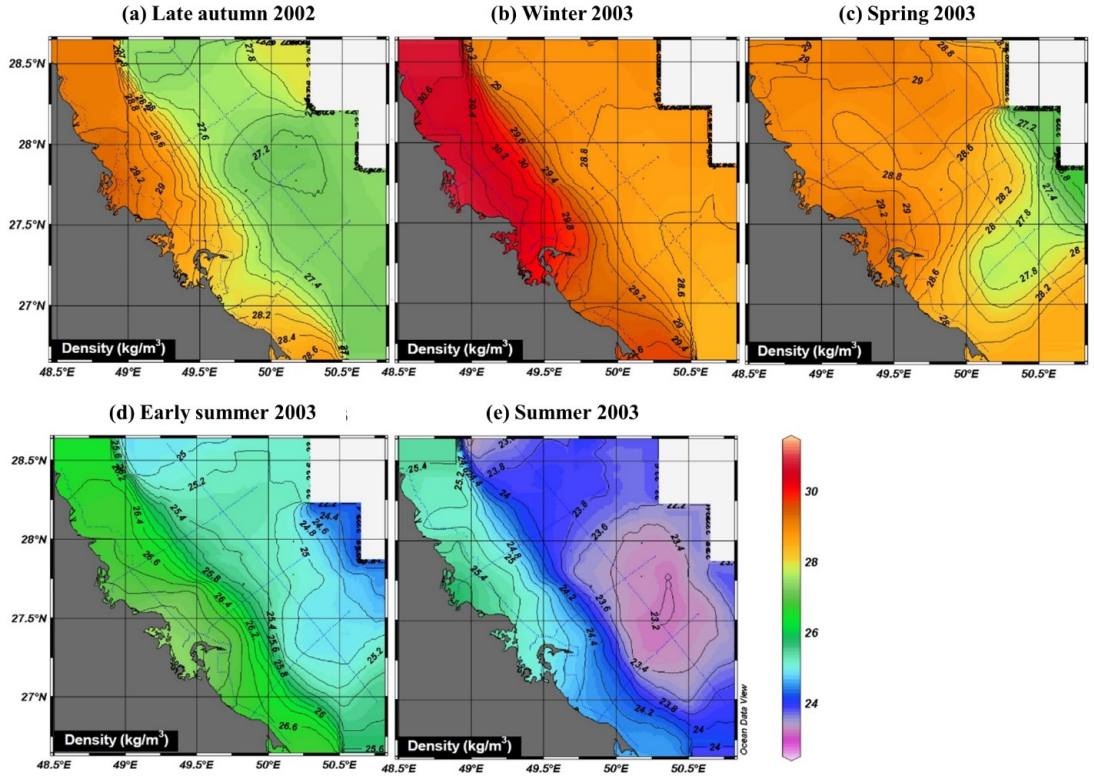

Figure 5. Spatial distribution of sea surface density in Saudi waters of the Gulf during late autumn 2002 (a), winter 2003 (b), spring 2003 (c), early summer 2003 (d) and summer 2003 (e).

The nearshore-offshore gradient in SST is weaker during summer, with a range of 34–35°C (Figure 3e). This is because of the thin surface layer formed in the Gulf during summer due to strong thermal stratification, during which the vertical mixing is weaker. The lowest annual mean wind speeds occur during late summer (August–September) (Aboobacker et al., 2021a), which further enhances the thermal stratification (Al-Ansari et al., 2022; Aboobacker et al., 2024). In an earlier study, John et al. (1990) reported an SST of 35.5°C, north of Abu Ali Island during summer. The slight difference in the maximum SST in this study could be due to the difference in the sampling periods. Spring exhibits a moderately low SST (around 21–22°C) in the northern offshore region of Saudi waters, compared to the nearshore (24–25°C) (Figure 3c). Whereas the opposite is true during late autumn, that is a relatively higher SST in the offshore (25–27°C) compared to the nearshore (22–24°C) (Figure 3a). The early summer is highly chaotic with no clear distinction of nearshore-offshore gradients of SST, while the SST is in the range 28–31°C (Figure 3d). This is a transformative stage from well-mixing to stratification. However, a high-temperature plume is visible on the central coast, affected by the excess heating in the shallow embayments compared to the adjacent regions (Joydas et al., 2011).

Nearshore-offshore variability in SSS is evident in all the seasons (Figure 4). A salty water flow toward the south from the northern end of the Saudi coast is fairly evident during summer, late autumn, and winter, which has interceded by a relatively low saline water inflow from offshore. A high saline water plume is apparent in the central coast, especially in the shallow embayments north of Jubail, with the strongest plumes identified during and early summer. This underscores the significance of the shallow bay systems in intensifying the salinity levels of the northern coast of Saudi Arabia. The offshore-nearshore ranges of SSS during the late autumn, winter, spring, early summer, and summer are 40.4–41.8, 40.6–41.6, 39.4–42.4, 38.2–42.8, and 38.6–42.2, respectively. John et al. (1990) measured the SSS along the northern coast of Saudi Arabia as low as 37.9 during spring, and attributed this to strong northwesterly winds and southeastward curents that brign low saline water from northern Gulf influenced by the freshwater discharge from Shatt-al-Arab river. However, our results does not show such a lower salinity along the northern coasts. This is because Shatt-al-Arab river was less active since 2000 compared to 90's due to various factors, including, dam construction, increased water usage from Tigris and Euphrates rivers and changes in rainfall patterns (Alosairi and Pokavanich, 2017). Interestingly, surface intrusion of low saline water has occurred in the offshore waters of Saudi Arabia with increasing order of intensity during spring, early summer, and summer, respectively. Yao and Johns (2010) identified that the extent of intrusion of IOSW into the Gulf is higher in summer than in winter. The salinity of IOSW present in the EEZ of Qatar during late summer has a salinity range of 38.8–40.2 (Elobaid et al., 2022). This is consistent with the low-salinity water plume that appeared in the Saudi offshore waters indicating that the IOSW, which was tracked through the Iranian coast (Swift and Bower, 2003) has an extension up to the Saudi waters, which was not reported before.

Similar to SSS, the SSD also exhibits distinct spatial and seasonal variability in Saudi waters (Figure 5). The nearshore region experiences higher SSD than the offshore region, with the highest offshore-nearshore gradient occurring during early summer (24.2–27.2 kg m^{-3}) and the lowest during winter (28.8–30.8 kg m^{-3}). The highest SSD occurred during winter (around 30.6 kg m^{-3}) and the lowest during summer (23.2 kg m^{-3}). The northern coast experiences the highest density in all the seasons due to the relatively high evaporation in the shallow embayments. The low-density plume in the offshore is more prevalent during summer, followed by early summer and spring. This clearly depicts the presence of a water mass in the offshore distinct from the coastal waters. The SSD variations in the nearshore regions during summer are more or less the same (roughly 1.6), which is consistent with the observations of Hunter (1984).

4.3 Vertical distribution of temperature, salinity and density

Vertical profiles of temperature, salinity, and density along the coastal and offshore transects show distinct seasonal and nearshore-offshore variations (Figures 6, 7 and 8). Vertical homogeneity in temperature, salinity, and density began in late autumn and became rigorous in winter, in both transects. In comparison, spatial variability exists between nearshore and offshore parameters during the above seasons, with relatively higher temperatures in the offshore and higher salinity and density in the nearshore. In both seasons, Transect A gets cooled easily due to the shallowness of the water and its proximity to the land, while the higher water depths and the intrusion of IOSW causes slow cooling at Transect B. The shallow depths of coastal waters facilitate the vertical transfer of heat resulting in a faster mixing and dilution (Yoshida et al., 1998). On the other hand, higher evaporation, shallow depth nature and the influence of discharged brine together enable a higher salinity and density at Transect A, while the low saline inflow of IOSW enables a relatively lower salinity and density at Transect B.

In the offshore, the thermal stratification began during spring, with a thermocline occurred at 15–20 m depths (<20°C) (Figure 6), whereas the salinity stratification occurred only in the southern part of the transect (Figure 7). This indicates that the fraction of brine persists in the offshore waters during spring, while the low saline IOSW influences the southern part. This effect is also evident in the density profile during spring with a thin surface

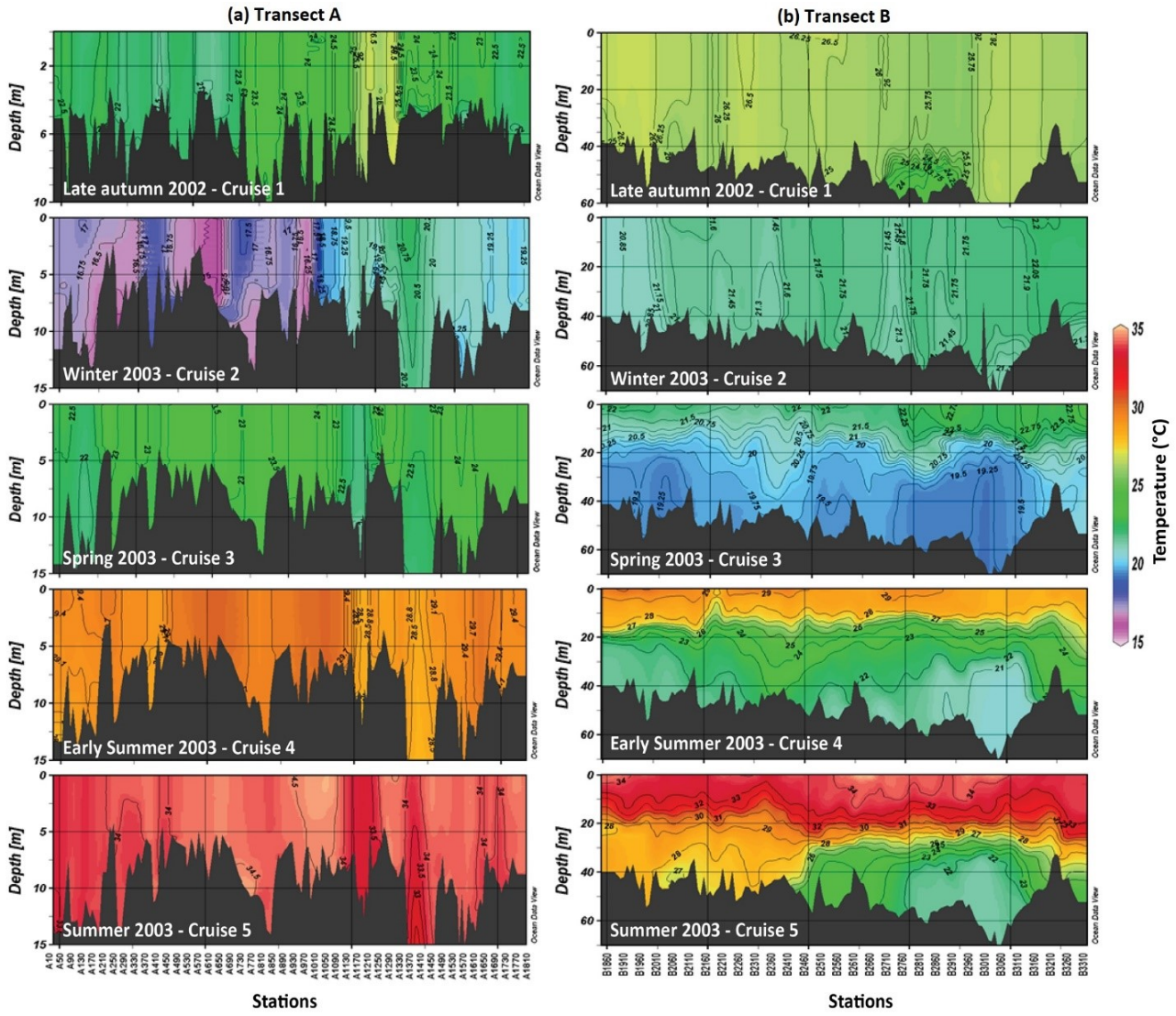

Figure 6. Vertical distribution of temperature along Transect A (a) and Transect B (b) during late autumn 2002, winter 2003, spring 2003, early summer 2003, and summer 2003.

layer (<5 m) in the north and a thick surface layer (up to 20 m) in the south (Figure 8). This stratification has been strengthened during early summer and became well pronounced during late summer. During early summer, the upper layer (up to 18 m) has a temperature range of 27–29°C, while the temperature drops down to 20–21°C in the bottom layer. Although the surface water is mostly contributed locally, signatures of IOSW with a lower salinity of around 39 are evident in the southern part of the transect (Figure 7). During late summer, the upper layer (up to 20 m) has heated quite extensively resulting in a temperature range of 31–35°C, while a thin mid-layer has been formed between 20 and 30 m depths in the southern part, with a temperature range of 26–30°C, while a bottom layer is formed below the mid-layer with a temperature range of 21–25°C. At the same time, the bottom layer in the northern part (20–40 m) has a temperature range of 27–30°C. This three-layer flow within the 60 m water column is peculiar to the Gulf. Such a 3-layer flow was reported earlier in the central Gulf, in the EEZ of Qatar during the late summer (Al-Ansari et al., 2022; Elobaid et al., 2022). Here, the surface temperature is uniformly distributed because of excess heating during summer, while the intrusion of IOSW is evident as reflected by the lower salinities of about 38.5–39.0. This increased salinity of the IOSW (basically below 37) is due to the estuarine nature of the flow, which mixes with the Gulf water. This water is present at up to 20 m water depth in the southern part, while only a few patches are visible in the northern part. In the northern part, the dispersion of brine induced high saline water might restrict the intrusion of IOSW, as reflected by the higher salinity in the northern part of the

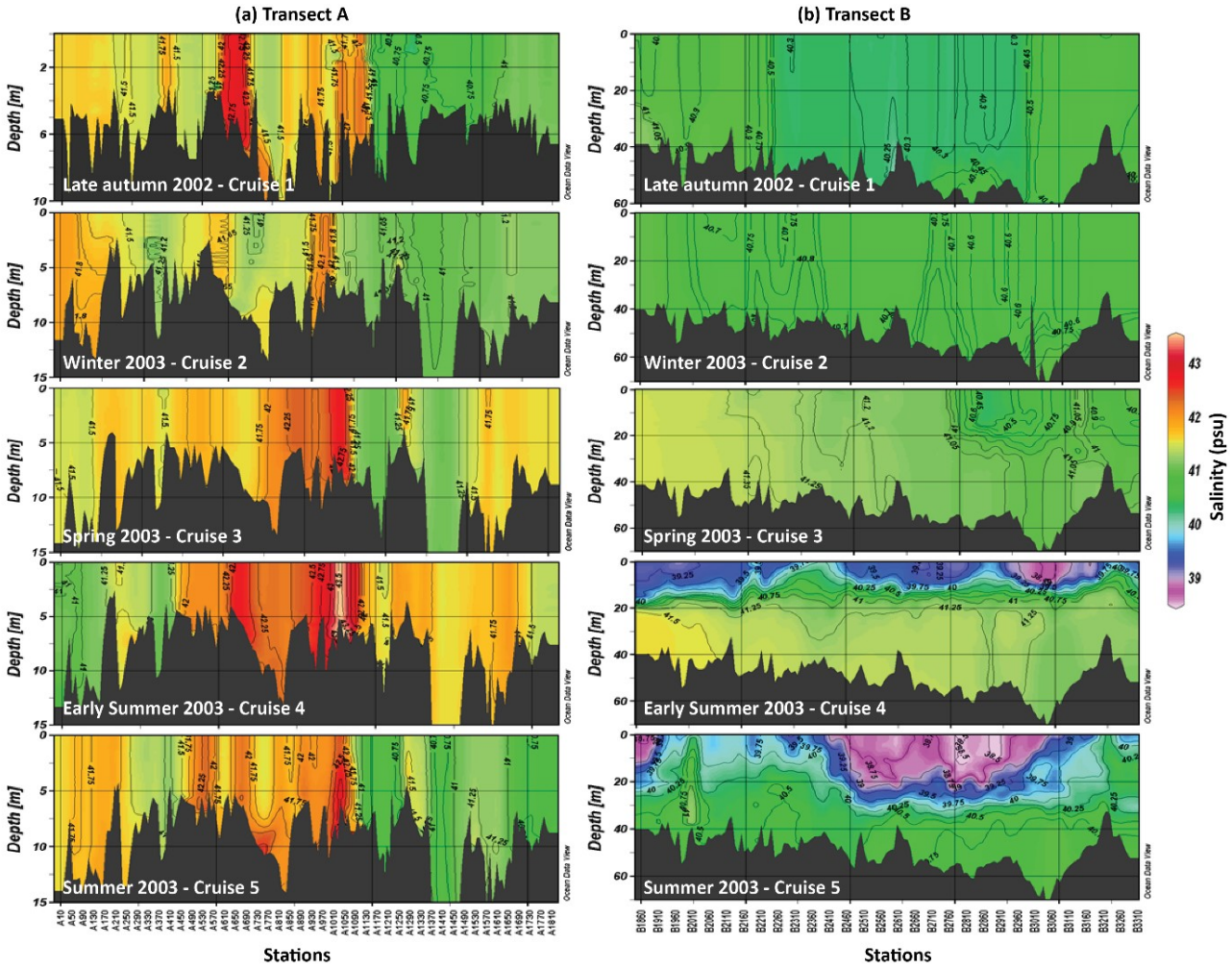

Figure 7. Vertical distribution of salinity along Transect A (a) and Transect B (b) during late autumn 2002, winter 2003, spring 2003, early summer 2003, and summer 2003.

coastal transect.

The cyclonic eddy in the northern Gulf is stronger during summer, and it has a prominent role in the Saudi offshore waters (Mussa et al., 2024). This shows that the intrusion of IOSW has a strong link with the magnitude of this eddy. In the coastal transect, the vertical temperature distribution is nearly homogenous during early and late summer (Figure 6), while horizontal variability in salinity exists due to the influence of brine discharges (Figure 7). The thin mid-layer water with a salinity of 40–41 formed in the Saudi offshore during summer is associated with the localized sinking of dense water, especially along the Arabian coast (Figure 8). The dense deep water identified in the Saudi offshore with a salinity of above 41 could be flown from the northern Gulf toward the Strait of Hormuz.

4.4 Water mass distribution

The vertical profiles in the cross-shore transects C, D, and E (northern, central, and southern, respectively, Figure 1) have been used to draw the T-S diagrams (Figure 9) and characterize the water masses in the Saudi Arabian waters of the Gulf. It reveals three distinct waters in this region, namely, Arabian Gulf Water (AGW), Bay Systems-induced Water (BSW), and IOSW. The AGW is also known as Persian Gulf Water (PGW). The temperature differences among the seasons result in slight gradients in their density distributions. However, the patterns are distinct throughout the year. Here the AGW is a deep water formed along the northwestern Gulf that flows through the southern deep part of the Strait of Hormuz (Johns et al., 2003). The BSW is a high saline water caused due to the shallow water embayments and by the brine discharge along the Saudi coast, as identified from the T-S diagram.

During late autumn and winter, the vertical mixing resulted in a constricted distribution of water masses (Figure 9a,b). The AGW is present in all the transects (C, D and E) with a density range of 27.0–29.0 kg m^{-3} during late autumn and 28.5–30.0 kg m^{-3} during winter. Meanwhile, the BSW with a density range of 30.0–32.5 kg m^{-3}

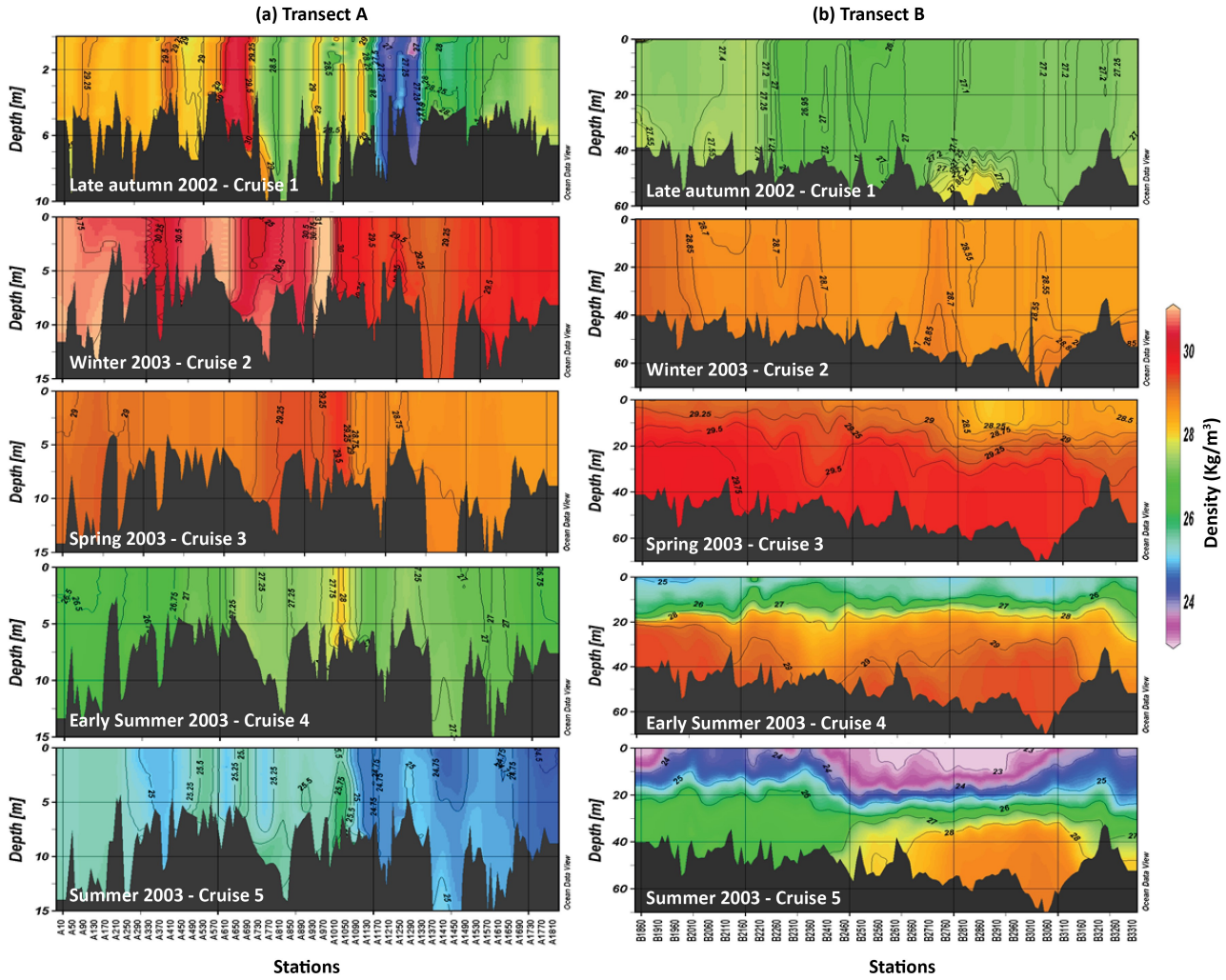

Figure 8. Vertical distribution of density along Transect A (a) and Transect B (b) during late autumn 2002, winter 2003, spring 2003, early summer 2003, and summer 2003.

is present only in the transect C and D during the above seasons. This water mass is more prominent in transect D, having a salinity gradient of about 1 with transect C. The BSW is mostly present in water depths less than 10 m, indicating its intense distribution in the coastal waters in the vicinity of the shallow embayments. This shows that the brine-induced impacts are limited to the coastal regions, while offshore regions are stable. This is consistent with the finding from the numerical modeling study of Ibrahim et al. (2020) that the Gulf maintains an equilibrium state with a stable annual basin-averaged salinity. Strong shamal winds during late autumn and winter enabled advection and dispersion of the elevated salinity at a faster rate compared to the other seasons, leading to a disappearance of BSW from transect E. Moreover, the features of IOSW have not been visible in the Saudi waters during the late autumn and winter, which could be attributed to the effects of prevailing shamal winds. Mussa et al. (2024) identified that the winter shamal winds oppose the Iranian Coastal Current (ICC) resulting in a reduction of monthly mean current speeds of the Gulf.

During spring, the density distribution of AGW is similar to that during winter. However, the density range of BSW is slightly dropped due to increased temperature: 28.5–30.0 kg m^{-3} and 28.5–31.0 kg m^{-3} at transects C and D, respectively (Figure 9c). Moreover, the BSW is present at transect E with limited salinity levels, as the stratification begins in spring. The interesting feature is the intrusion of IOSW during this season, which is more evident in transects D and E, while a small patch is observed in transect C. This has predominantly a density level of 26.5–28.0 kg m^{-3}. This is the first time the presence of IOSW has been reported in the Saudi waters of the Gulf with observational evidence, especially in the intermediate-shallow waters. The intrusion has been further strengthened during early summer (Figure 9d), as the stratification becomes stronger. The thin surface layer formed during this season could enable a fast intrusion of IOSW along with the

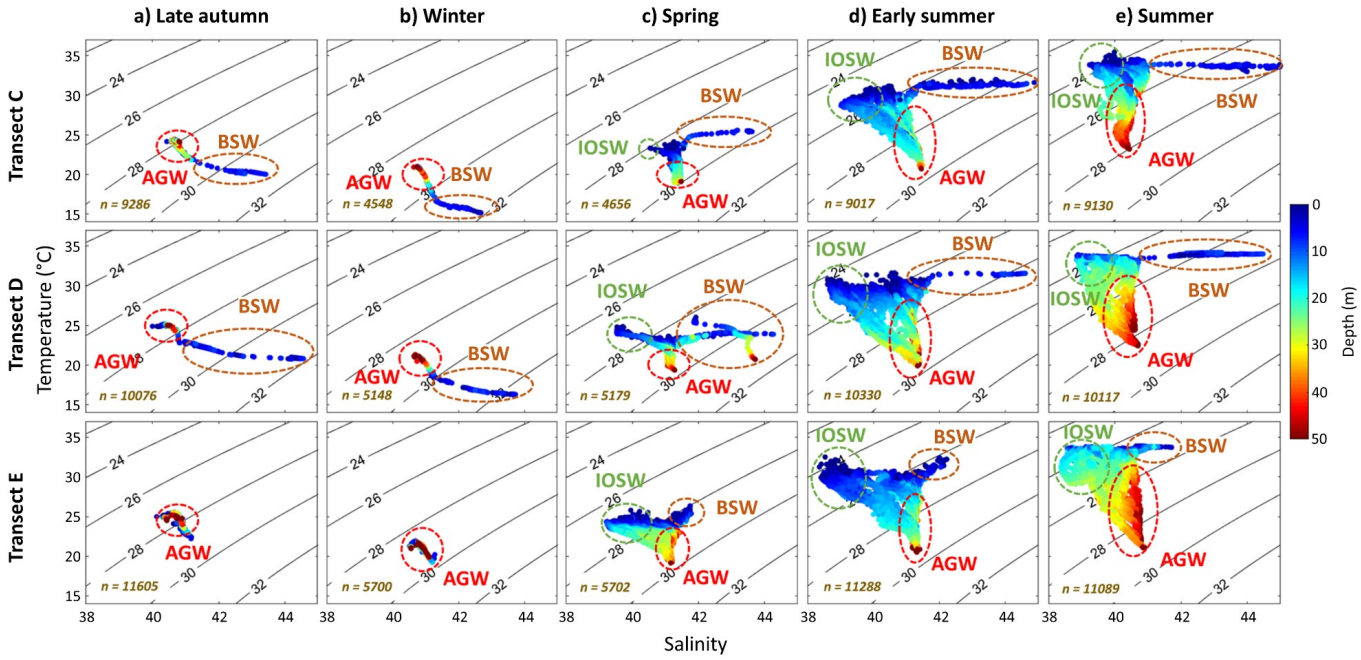

Figure 9. T-S diagrams of north, center, and south cross-shore transects in Saudi waters of the Gulf during late autumn 2002 (a), winter 2003 (b), spring 2003 (c), early summer 2003 (d), and summer 2003 (e). Color variations indicate water depths.

increased intensity of ICC (Mussa et al., 2024). The density levels of IOSW during this season are 23.5–26, 24–26.5, and 25–26.5 kg m^{-3}, respectively, at transects E, D, and C, with decreasing order of its intensity as it progresses toward the north. The progression of IOSW during early summer is mostly through the intermediate and shallow waters of the Saudi coast as indicated by the respective depths. During summer, there is a pattern change in the progression of IOSW, as evident from their presence in the deep-water and intermediate-water locations, especially at transects D and E (Figure 9e). The density levels of IOSW during this season are 23.0–25.0 kg m^{-3} at transects D and E and 23.5–25.0 kg m^{-3} at transect C.

The AGW is widely scattered during early summer, and mostly appears in the intermediate layers (Figure 9d). Whereas it sinks further during the summer and appeared in the bottom layer (Figure 9e). This is due to the development of a well-structured bottom layer with reduced thickness due to strong stratification (Al-Ansari et al., 2022). Such a development has led to the formation of summer hypoxia in the bottom layer (>47 m) of the central Gulf, where the water depth was about 67 m (Al-Ansari et al., 2015). In the transects we analyzed, the maximum depth is about 60 m. So far, there are no reports of hypoxia in the Saudi waters of the Gulf. The BSW has been elongated further during early summer and summer compared to other seasons. This is primarily due to the increase in the intensity of ACC (Mussa et al., 2024), which has increased the chances of spreading the brine to farther distances, especially toward the south. The sinking of BSW to a depth of about 20 m is evident in transect E during summer.

The above water masses pose a detailed picture of the Gulf's dynamic and complex nature. The formation of these water masses took place within the Gulf, and therefore, rapid variations in temperature and salinity characteristics of each water masses is evident in the measurements. The temperature and salinity signatures of IOSW gradually disappear as it flows northward due to surface heating and higher evaporation. The dense water that sinks in the northern Gulf ultimately leads to the formation of AGW, which flows out through the Strait of Hormuz as a well-oxygenated water, and has been detected in the far areas of the Indian Ocean (Prasad et al., 2001; Jain et al., 2017; L'Hégaret et al., 2021). The Gulf of Salwa Water, another prominent water previously reported in the Gulf with salinities often reaching above 52 (John et al., 1990), is not evident along the transects. This is mainly due to the opposing surface currents (Alosairi and Pokavanich, 2017; Mussa et al., 2024) inhibiting the northward propagation of the Gulf of Salwa water. The inflow from the Indian Ocean to the Gulf is equally important as the outflow from the Gulf, because it stabilizes the Gulf by maintaining an equilibrium salinity. Recent changes in the Arabian Sea salinity and temperature may reflect in the inflow characteristics including its northward extension. This may in turn, affect the overturning circulations of the Gulf and the deep-water outflow. This needs to be investigated further with more recent datasets.

5. Summary and conclusions

The study utilized past measurements (during 2002–2003) of temperature, salinity, and density at five transects in the Saudi Arabian waters of the Gulf, and analyzed their spatial and temporal variability. The northern coast is characterized by Tanajib-Manifa-Ras Al Khair- Dohat Ad Dafi shallow embayments, and the measurements demonstrated that they cause significant variations in salinity and temperature along this region. The obstruction of northward flow of brine-induced water from the desalination plants by the Abu Ali Island also caused the elevated salinity levels in the vicinity of the island. The offshore-nearshore gradients of SSS during the late autumn, winter, spring, early summer, and summer are 40.4–41.8, 40.6–41.6, 39.4–42.4, 38.2–42.8, and 38.6–42.2, respectively. This has been supported by the offshore-nearshore gradient in SSD, highest during early summer (24.2–27.2 kg m^{-3}) and lowest during winter (28.8–30.8 kg m^{-3}). While vertical homogeneity in temperature and salinity was present during late autumn and winter, the spring, early summer, and summer exhibited thermal stratification with a thermocline developed at 15–20 m below the surface. Late summer marked the formation of 3 layers (surface, subsurface, and bottom) with distinct temperature, salinity, and density. This is peculiar to the Gulf considering the shallowness of the basin, and this has been reported for the first time in the Saudi waters from in situ measurements.

Three distinct water masses, AGW, BSW, and IOSW were identified in the Saudi waters. AGW prevailed in the entire Saudi waters throughout the year, with considerable seasonal variations. The intrusion of IOSW began during spring, with a gradual progressiveness from south to north, while it attained a well-defined pattern during early summer and summer. A remarkable presence of BSW was found along the central and northern transects in all the seasons, but with a prolonged salinity distribution during early summer and summer. The intensified ACC during summer enhanced the southward transport of BSW, which resulted in the sinking of water mass at the southern transect to a depth of above 20 m. This study underscores the significance of the shallow embayments along the northern coast of Saudi Arabia in intensifying the salinity levels in their proximity, while relatively low salinity persists in other areas. The three water masses and associated transports have a significant role in maintaining the salinity equilibrium of the Gulf; however, recent changes in hydrography and water mass characteristics need to be investigated through repeated measurements and numerical modelling to elucidate further on the decadal variability and its driving mechanisms, including the role of climate change, which we aim as our future scope of study.

We acknowledge that the data used in this study is older than two decades. During this period there have been substantial changes in coastal developments along the coastal areas, including land reclamation, construction of marinas, ports and desalination plants. These developments could have altered the bathymetry and coastal morphology, which in turn affect the coastal circulation and hydrographic features. In addition, increased capacity of desalination in recent years across the region could have added more salinity/density to the water in the vicinity of the outfalls. Notwithstanding these limitations, the data presented in this study can be considered as a strong historical basis, and can be compared with the most recent or future measurements to study the decadal changes in hydrography and water masses along the Saudi Arabian coast.

Acknowledgements

We thank the Applied Research Center for Environment and Marine Studies (ARCEMS) at the Research & Innovation of the King Fahd University of Petroleum and Minerals, Dhahran, Saudi Arabia, for providing research facilities and the Marine Group of ARCEMS for performing the fieldwork. We express our sincere thanks to the General Authority of Meteorology and Environmental Protection, Saudi Arabia, and the Saudi Company for Environmental Works Ltd. for their constant support. We also thank M/S Al-Gosaibi for providing services of their Oceanographic Vessel. The authors from Qatar University thanks Prof. Hamad Al-Saad Al-Kuwari, Director, Environmental Science Center for his constant support. This collaborative research has been framed under the UNESCO Chair in Marine Sciences at Qatar University. The third author gratefully acknowledges the grant QUPD-ESC-24/25-1449 for the P-DOC funding.

Data availability statement

The in situ data used in this study are made freely available through Figshare (https://doi.org/10.6084/m9.figshare.29974675.v1).

Conflict of interest

None declared.

References

Aboobacker, V.M., Hasna, V.M., Al-Ansari, E.M.A.S., Vethamony, P., 2024. *Nearshore hydrography along the coast of Doha, central Arabian Gulf*. Coastal Res. 113 (Sp. Iss.), 422–426.

Aboobacker, V.M., Samiksha, S.V., Veerasingam, S., Al-Ansari, E.M.A.S., Vethamony, P., 2021c. *Role of shamal and easterly winds on the wave characteristics off Qatar, Central Arabian Gulf*. Ocean Eng. 236, 109457.

Aboobacker, V.M., Shanas, P.R., Al-Ansari, E.M.A.S., Sanil Kumar, V., Vethamony, P., 2021b. *The maxima in northerly wind speeds and wave heights over the Arabian Sea, the Arabian/Persian Gulf and the Red Sea derived from 40 years of ERA5 data*. Climate Dynam. 56, 1037–1052.

Aboobacker, V.M., Shanas, R.P, Veerasingam, S., Al-Ansari E.M.A.S., Sadooni, F.N., Vethamony, P., 2021a. *Long-Term Assessment of Onshore and Offshore Wind Energy Potentials of Qatar*. Energies 14, 1178–1178.

Al-Abdulkader, K.A., Loughland, R.A., Qurban, M.A., 2019. *Ecosystems and biodiversity of the Arabian Gulf. Saudi Arabian waters. In: Fifty Years of Scientific Research*. Publi. Saudi Aramco and King Fahd Univ. Petrol. Min., Dhahran, Saudi Arabia, 624 pp.

Al-Ansari, E.M., Husrevoglu, Y.S., Yigiterhan, O., Youssef, N., Al-Maslamani, I.A., Abdel-Moati, M.A. Vethamony, P., 2022. *Seasonal variability of hydrography off the east coast of Qatar, central Arabian Gulf*. Arabian J. Geosci. 15 (22), 1659. https://doi.org/10.1007/s12517-022-10927-4

Al-Ansari, E.M., Rowe, G., Abdel-Moati, M.A.R., Yigiterhan, O., Al-Maslamani, I., Al-Yafei, M.A., Al-Shaikh, I., Upstill-Goddard, R., 2015. *Hypoxia in the central Arabian Gulf Exclusive Economic Zone (EEZ) of Qatar during summer season*. Estuar. Coast. Shelf Sci. 159, 60–68.

Alosairi, Y., Al-Salem, S.M., Al Ragum, A., 2020. *Three-dimensional numerical modelling of transport, fate and distribution of microplastics in the northwestern Arabian/Persian Gulf*. Mar. Pollut. Bull. 161, 111723. https://doi.org/10.1016/j.marpolbul.2020.111723

Alosairi, Y., Pokavanich, T., 2017. *Seasonal circulation assessments of the northern Arabian/Persian Gulf*. Mar. Pollut. Bull. 116 (1–2), 270–290.

Asharaf, M., Aboobacker, V.M., Abdulla, C.P., Joydas, T.V., Manikandan, K., Rafeeq, M., Al-Suwailem, A., Vethamony, P., 2025. *In situ Data of different seasons from the Saudi waters of the Arabian Gulf*. Figshare, dataset. https://doi.org/10.6084/m9.figshare.29974675.v1

de Marez, C., L'Hégaret, P., Morvan, M., Carton, X., 2019. *On the 3D structure of eddies in the Arabian Sea*. Deep-Sea Res. Pt. I, 150, 103057.

Elobaid, E.A., Al-Ansari, E.M.A.S., Yigiterhan, O., Aboobacker, V.M., Vethamony, P., 2022. *Spatial variability of summer hydrography in the central Arabian Gulf*. Oceanologia, 64 (1), 75–87.

Ghaemi, M., Gholamreza, M., Samad, H., Sara, G., 2022. *Spatial and temporal characterizations of seawater quality on marine waters area of the Persian Gulf*. Reg. Stud. Mar. Sci. 53, 102407. https://doi.org/10.1016/j.rsma.2022.102407

Hanert, E., Aboobacker, V.M., Veerasingam, S., Dobbelaere, T., Vallaeys, V., Vethamony, P., 2023. *Multiscale ocean modelling system for the central Arabian/Persian Gulf: From regional to structure scale circulation patterns*. Estuar. Coast. Shelf Sci. 282, 108230. https://doi.org/10.1016/j.ecss.2023.108230

Hassanzadeh, S., Hosseinibalam, F., Rezaei-Latifi, A., 2011. *Numerical modelling of salinity variations due to wind and thermohaline forcing in the Persian Gulf*. Appl. Math. Model. 35 (3), 1512–1537. https://doi.org/10.1016/j.apm.2010.09.029

Hunter, J.R., 1986. *The physical oceanography of the Arabian Gulf: a review and theoretical interpretation of previous observations*. [In:] *First Gulf Conference on Environment and Pollution* 7-9, February (1982), Kuwait, R. Halway (Ed).

Hunter, J.R., 1984. *A review of the residual circulation and mixing process in the KAP region*. [In:] *Oceanographic modelling of the Kuwait Action Plan Region*, M.I. El-Sabh (Ed.), UNESCO Rep. Mar. Sci., 28, 37–45.

Ibrahim, H.D., Xue, P., Eltahir, E.A., 2020. *Multiple salinity equilibria and resilience of Persian/Arabian Gulf basin salinity to brine discharge*. Front. Mar. Sci. 7, 573. https://doi.org/10.3389/fmars.2020.00573

Jain, V., Shankar, D., Vinayachandran, P. N., et al. 2017. *Evidence for the existence of Persian Gulf water and Red Sea water in the Bay of Bengal*. Clim. Dynam. 48, 3207–3226. https://doi.org/10.1007/s00382-016-3259-4

John, V.C., Coles, S.L., Abozed, A.I., 1990. *Seasonal cycles of temperature, salinity and water masses of the western Arabian Gulf*. Oceanologica Acta 13 (3), 273–281.

Johns, W.E, Jacob, G.A., Kindle, J.C., Murray, S.B., Carron, M., 1999. *Arabian marginal seas and gulfs*. Workshop Rep., Stennic Space Centre, University of Miami RSMAS Technical Report 2000-01, 11–13 May, Mississippi.

Johns, W.E., Yao, F., Olson, D.B., Josey, S.A., Grist, J.P., Smeed, D.A., 2003. *Observations of seasonal exchange through the Straits of Hormuz and the inferred heat and freshwater budgets of the Persian Gulf*. J. Geophys. Res. 108 (C12).

Joydas, T.V., Krishnakumar, P.K., Qurban, M.A., Ali S.M., Al-Suwailem, A., Al-Abdulkader, K., 2011. *Status of macrobenthic community of Manifa–Tanajib Bay System of Saudi Arabia based on a once-off sampling event*. Mar. Pollut. Bull. 62, 1249–1260.

Joydas, T.V., Qurban M.A., Borja, A., Manokaran, S., Manikandan, K.P., Lotfi, J.R., Garmendia J.M., Asharaf T.T.M., Ayranci, K., Shemsi, A.M, Mohammed, S., Basali, A.U., Panickan, P., Nazeer, Z., Lyla, P.S., Khan, S.A., Krishnakumar, P.K., 2023. *Ecological status of macrobenthic communities in the Saudi waters of the western Arabian Gulf*. Reg. Stud. Mar. Sci. 57, 102751, 2352–4855. https://doi.org/10.1016/j.rsma.2022.102751

Joydas, T.V., Qurban, M.A., Manikandan, K.P., et al. 2015. *Status of macrobenthic communities in the hypersaline waters of the Gulf of Salwa, Arabian Gulf*. J. Sea Res. 99, 34–46. https://doi.org/10.1016/j.seares.2015.01.006

Kämpf, J., Sadrinasab, M., 2006. *The circulation of the Persian Gulf: a numerical study*. Ocean Sci. 2 (1), 27–41. https://doi.org/10.5194/os-2-27-2006

KFUPM/RI., 1990a. *Final Report: Aramco Sustaining Research Project – Environmental Studies*, Vol. VI, Oceanographic Investigation – Coastal and Offshore Hydrog-

raphy. Prepared for Saudi Aramco by the Water Resources and Environment Division, Research Institute, King Fahd University Petroleum and Minerals, Dhahran, Saudi Arabia, Report Project No. 24079.

KFUPM/RI., 1990b. *Final Report: Aramco Sustaining Research Project – Environmental Studies*, Vol. VII, Hydrodynamic Models for Wind-Driven and Tidal Circulation in the Arabian Gulf. Prepared for Saudi Aramco by the Water Resources and Environment Division, Research Institute, King Fahd University Petroleum and Minerals, Dhahran, Saudi Arabia, Report Project No. 24079.

KFUPM/RI., 1990c. *Final Report: Aramco Sustaining Research Project – Environmental Studies*, Vol. VIII, Simulation Models of Pollutant Fate and Transport in the Arabian Gulf. Prepared for Saudi Aramco by the Water Resources and Environment Division, Research Institute, King Fahd University Petroleum and Minerals, Dhahran, Saudi Arabia, Report Project No. 24079.

Le Provost, C., 1983. *Models for tides in the KAP region*. [In:] *Oceanographic Modeling of the Kuwait Action Plan Region*, M.I. El-Sabh (Ed), Vol. 28, UNESCO Rep. Mar. Sci., Paris, 37–45.

L'Hégaret, P., Marez, C.D., Morvan, M., Meunier, T., Carton, X., 2021. *Spreading and vertical structure of the Persian Gulf and Red Sea outflows in the northwestern Indian Ocean*. J. Geophys. Res. 126 (4), e2019JC015983. https://doi.org/10.1029/2019JC015983

Madah, F., Gharbi, S.H., 2022. *Numerical simulation of tidal hydrodynamics in the Arabian Gulf*. Oceanologia 64 (2), 327–345.

Marin, M., Bindoff, N.L., Feng, M., Phillips, H.E., 2021. *Slower long-term coastal warming drives dampened trends in coastal marine heatwave exposure*. J. Geophys. Res. 126, e2021JC017930. https://doi.org/10.1029/2021JC017930

Mussa, A.A., Aboobacker, V.M., Abdulla, C.P., Hasna, V.M., Al-Ansari, E.M., Vethamony, P., 2024. *A climatological overview of surface currents in the Arabian Gulf with special reference to the Exclusive Economic Zone of Qatar*. Int. J. Climatol. 44 (13), 4677–4693.

Prasad, T.G., Ikeda, M., Kumar, S.P., 2001. *Seasonal spreading of the Persian Gulf Water mass in the Arabian Sea*. J. Geophys. Res. 106 (C8), 17059–17071. https://doi.org/10.1029/2000JC000480

Pokavanich, T., Polikarpov, I., Lennox, A., et al. 2013. *Comprehensive investigation of summer hydrodynamic and water quality characteristics of desertic shallow water body: Kuwait Bay*. J. Coast. Dynam. 12 (2), 1253–1264.

Pous, S., Carton, X., Lazure, P., 2013. *A process study of the wind-induced circulation in the Persian Gulf*. Open J. Mar. Sci. 3 (1), 1–11.

Rakib, F., Al-Ansari, E.M., Husrevoglu, Y.S., Yigiterhan, O., Al-Maslamani, I., Aboobacker, V.M., Vethamony, P., 2021. *Observed variability in physical and biogeochemical parameters in the central Arabian Gulf*. Oceanologia 63 (2), 227–237. https://doi.org/10.1016/j.oceano.2020.12.003

Reynolds, R.M., 1993. *Physical oceanography of the Gulf, Strait of Hormuz and the Gulf of Oman – Results from the Mt. Mitchell Expedition*. Mar. Pollut. Bull. 27, 35–37.

Roy, P., Rao, I.N., Martha, T.R., Kumar, K.V., 2022. *Discharge water temperature assessment of thermal power plant using remote sensing techniques*. Energy Geosci. 3 (2), 172–181. https://doi.org/10.1016/j.engeos.2021.06.006

Schlitzer, R., 2003. *Ocean Data View (ODV) mp-version 1.4* (odvmp_1.4_w32.zip).

Sheppard, C.R.C., 1993. *Physical environment of the Gulf relevant of marine pollution: An over view*. Mar. Pollut. Bull. 27, 3–8.

Siddig, N.A., Al-Subhi, A.M., Alsaafani, M.A., 2019. *Tide and mean sea level trend in the west coast of the Arabian Gulf from tide gauges and multi-missions satellite altimeter*. Oceanologia 61 (4), 401–411.

Swift, S.A., Bower, A.S., 2003. *Formation and circulation of dense water in the Persian/Arabian Gulf*. J. Geophys. Res. 108 (1), 3004.

Thoppil, P.G., Hogan, P.J., 2010. *A modeling study of circulation and eddies in the Persian Gulf*. J. Phys. Oceanogr. 40 (9), 2122–2134.

Veerasingam, S., Al-Khayat, J.A., Aboobacker, V.M., Hamza, S., Vethamony, P., 2020a. *Sources, spatial distribution and characteristics of marine litter along the west coast of Qatar*. Mar. Pollut. Bull. 159, 111478. https://doi.org/10.1016/j.marpolbul.2020.111478

Veerasingam, S., Al-Khayat, J.A., Haseeba, K.P., Aboobacker, V.M., Hamza, S., Vethamony, P., 2020b. *Spatial distribution, structural characterization and weathering of tarmats along the west coast of Qatar*. Mar. Pollut. Bull. 159, 111486.

Veerasingam, S., Ranjani, M., Venkatachalapathy, R., Bagaev, A., Mukhanov, V., Litvinyuk, D., Mugilarasan, M., Gurumoorthi, K., Guganathan, L., Aboobacker, V.M., Vethamony, P., 2021a. *Contributions of Fourier transform infrared spectroscopy in microplastic pollution research: A review*. Crit. Rev. Environ. Sci. Tech. 51 (22), 2681–2743. https://doi.org/10.1080/10643389.2020.1807450

Veerasingam, S., Vethamony, P., Aboobacker, V.M. Giraldes, A.E., Dib, S., Al-Khayat, J.A., 2021b. *Factors influencing the vertical distribution of microplastics in the beach sediments around the Ras Rakan Island, Qatar*. Environ. Sci. Pollut. Res. 28, 34259–34268. https://doi.org/10.1007/s11356-020-12100-4

Yao, F., Johns, W.E., 2010. *A HYCOM modeling study of the Persian Gulf: 1. Model configurations and surface circulation*. J. Geophys. Res. 115, C11017. https://doi.org/10.1029/2009JC005781

Yoshida, J., Matsuyama, M., Senjyu, T., et al. 1998. *Hydrography in the RSA during the RT/V Umitaka-Maru cruises*.

[In:] *Offshore Environment of the ROPME Sea Area after the War-Related Oil Spill – Results of the 1993–94 Umitaka-Maru Cruise*, Otsuki, A., Abdeulraheem, M., Reyolds, M. (Eds.), Terra Sci. Publ. Company, Tokyo, 1–22.